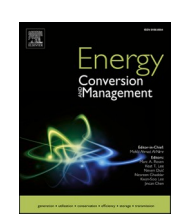
FISEVIER

Contents lists available at ScienceDirect

## **Energy Conversion and Management**

journal homepage: www.elsevier.com/locate/enconman





# Optimized schemes of enhanced shale gas recovery by CO<sub>2</sub>-N<sub>2</sub> mixtures associated with CO<sub>2</sub> sequestration

Haoming Ma  $^a$ , Yun Yang  $^{b,1,*}$ , Yuming Zhang  $^a$ , Ziyan Li  $^b$ , Kai Zhang  $^a$ , Zhenqian Xue  $^a$ , Jie Zhan  $^c$ , Zhangxin Chen  $^{a,1}$ 

- a Department of Chemical & Petroleum Engineering, University of Calgary, 2500 University Drive NW, Calgary, Alberta T2N 1N4, Canada
- <sup>b</sup> Department of Geoscience, University of Calgary, 2500 University Drive NW, Calgary, Alberta T2N 1N4, Canada
- <sup>c</sup> School of Petroleum Engineering, Xi'an Shiyou University, 710065, China

#### ARTICLE INFO

 $\begin{tabular}{ll} $Keywords:$\\ $CO_2$-$N_2$ flooding\\ $ESGR$\\ $CO_2$ sequestration\\ $Optimization$\\ \end{tabular}$ 

#### ABSTRACT

In response to the growing demand for  $CO_2$  mitigation and unconventional natural gas, the oil and gas industry is researching for the viability to enhance shale gas recovery (ESGR) and sequester  $CO_2$  in depleted reservoirs. Previous research has shown that a  $CO_2$ - $N_2$  mixture can be employed as a desired injection fluid to concurrently address both industrial issues. Due to the infancy of ESGR operations, there is no thorough knowledge of field-level optimized strategies using  $CO_2$ - $N_2$  for the ESGR associated with  $CO_2$  sequestration. In this study, the commercial reservoir simulator GEM and CMOST by CMG were adopted to conduct  $\sim 120$  simulation scenarios based on the Barnett shale formation in order to comprehend the impacts of three dominating operational parameters and propose the corresponding solutions. This study reveals four major findings. Firstly, a larger  $N_2$  concentration corresponds to a better recovery factor of shale gas but a shorter breakthrough time that causes the worse  $CO_2$  storage performance. Secondly, an injection rate is initially proportional to the shale gas recovery and  $CO_2$  storage performance but beyond a threshold rate, it can inversely affect both outcomes. Thirdly, the influence of a soaking period is limited in a short term and negligible in a long term for both ESGR and  $CO_2$  sequestration. Lastly, by selecting an appropriate combination of an injection rate and a  $CO_2$ - $N_2$  ratio, the income of a project can significantly be improved by 22 % under the current carbon tax policy. This study provides shale gas operators with a guideline for implementing large-scale ESGR projects employing  $CO_2$ - $N_2$  mixtures.

## 1. Introduction

According to a recent report from International Energy Agency (IEA), the demand for natural gas is increasing by 430 billion cubic meters (bcm) between 2021 and 2030 while the conventional gas production will decline by around 740 bcm by 2050, and the natural gas demand will reach 5,100 bcm which is 30 % much higher than today [1]. The rising natural gas demand and the depletion of conventional gas reserves promoted the petroleum industry to shift its direction to unconventional resources. Shale gas is one of the most reliable unconventional natural gas resources thanks to the commercialized revolution of multi-stage hydraulic fracturing and horizontal drilling development [2].

However, the current matured recovery techniques can only recover about 30 % original gas in place (OGIP) owing to the complex trapping and adsorption mechanisms of methane [3–9]. On the other hand, a rising demand of energy triggered the increasing greenhouse gas emissions which accelerated the climate change. According to IEA, the annual energy-related and industrial  $CO_2$  emissions are predicted to achieve 36 Gt by 2030, which would lead to 2.7°C global temperature rising by 2100 with 50 % probability [10]. As Intergovernmental Panel on Climate Change (IPCC) proved, permanently sequestrating  $CO_2$  in the subsurface is a promising solution to mitigate the  $CO_2$  emissions in the current energy transition and linear carbon economy [11,12]. In the oil and gas industry, an application of  $CO_2$  injection since the 1980 s can not

Abbreviations: bcm, billion cubic meters; BHP, Bottomhole pressure; ESGR, Enhanced shale gas recovery; HnP, Huff and Puff; HCPV, hydrocarbon pore volume; IPCC, Intergovernmental Panel on Climate Change; IEA, International Energy Agency; MMSCF, million standard cubic feet; OGIP, Original gas in place; RF, Recovery factor; UF, Utilization factor.

E-mail addresses: yun.yang2@ucalgary.ca, yun.yang@ucalgary.ca (Y. Yang), zhachen@ucalgary.ca (Z. Chen).

Corresponding author.

<sup>&</sup>lt;sup>1</sup> The two authors have the same contribution to this study.

only increase the hydrocarbon recovery factor (RF) but also mitigate the  $\mathrm{CO}_2$  emissions of the industry by storing  $\mathrm{CO}_2$  to depleted reservoirs [13–25]. In recent years, studies illustrated that it is feasible to deploy  $\mathrm{CO}_2$  to enhanced shale gas recovery (ESGR) due to pressure gradient changes and competitive adsorption mechanisms [26–33].

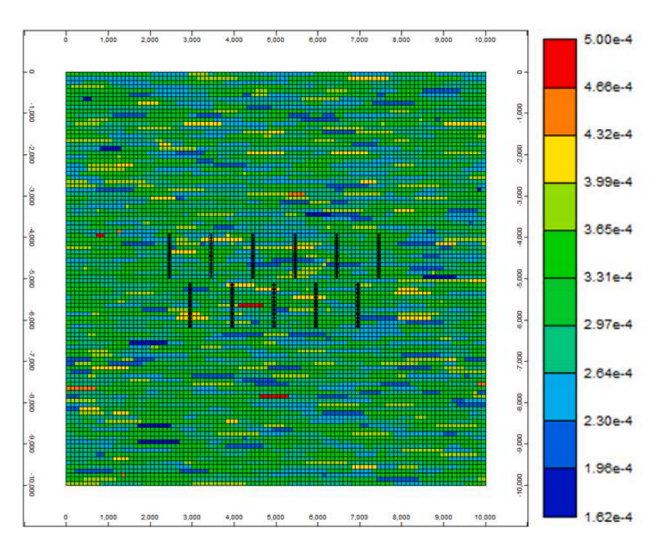
To our knowledge, only few known CO2-ESGR projects worldwide are still in a primary recovery stage [34]. Unlike a primary recovery process which is driven mainly by pressure depletion after hydraulic fracturing, CO2-N2-ESGR can both increase a pressure gradient to overcome a low-permeability constraint and free up methane in an absorbed phase so that the RF can be significantly improved [35-37]. It has also been demonstrated that closure of the fracture also plays an important role in fluid recovery [38,39]. Additionally, the competitive gas adsorption follows Langmuir isotherms assuring that absorbed methane can be recovered [2]. The preferentially adsorption capacities of N<sub>2</sub>, CH<sub>4</sub> and CO<sub>2</sub> on shale are in a ratio of 2:3:15 [37]. Injecting a mixture of high affinity gas (i.e., CO2) and low affinity gas (i.e., N2) can increase the RF of CH<sub>4</sub> because the absorption of CH<sub>4</sub> can be replaced by CO<sub>2</sub> due to the competitive adsorption mechanism and the partial pressure of CH<sub>4</sub> declined to promote CH<sub>4</sub> to a desorption state owing to N<sub>2</sub> injection. Theoretically, both CO<sub>2</sub>-ESGR and N<sub>2</sub>-ESGR can have a significant impact on ESGR, but injecting CO<sub>2</sub> leads to low mobility at the reservoir conditions while injecting N2 always results in extremely short breakthrough time [34]. Thus, the injection of a CO<sub>2</sub>-N<sub>2</sub> mixture can potentially extract more shale gas while avoiding individual drawbacks [34]. Furthermore, an application of CO2-N2 requires less separation energy from a flue gas which reduces the cost of a gas source. The research status of utilizing a CO2-N2 mixture for the ESGR purpose is still in an infancy stage. Prior to this work, experimental and numerical studies have proven that an application of a CO<sub>2</sub>-N<sub>2</sub> mixture can achieve the goals of ESGR and CO<sub>2</sub> sequestration simultaneously by determining an optimal injectivity ratio [34]. Li and Elsworth proved that a mixture of  $CO_2$ - $N_2$  can increase the shale gas RF by  $\sim$  20 % by controlling a component ratio [34]. On the other hand, CO2 can be sequestrated in shale gas reservoirs mainly dominated by structural trapping and adsorption mechanisms [11,40]. Once shale gas is produced, a volume can be created to store CO<sub>2</sub>, and the competitive adsorption of CO<sub>2</sub>/CH<sub>4</sub> allows a greater CO<sub>2</sub> storage capacity in an absorbed phase [26,41-43]. However, the operating schemes were not well-established for CO<sub>2</sub>-N<sub>2</sub>-ESGR projects as they will directly impact the reservoir performance as well as the feasibility of CO<sub>2</sub> storage in shale gas reservoirs.

In this research, we developed a series of scenario studies based on the numerical simulator CMG-GEM to study the reservoir performance of CO $_2$ -N $_2$ -ESGR from both methane recovery and CO $_2$  sequestration perspectives. Optimal operating schemes and optimal gas ratios of CO $_2$ -N $_2$  were selected based on different injection schemes including simultaneous flooding and cyclic flooding. The rest of this paper is structured as follows: Section 2 describes the basic reservoir properties of the numerical model and the selection of performance indicators. Section 3 discusses the results for all scenarios (~120 simulation case) as well as the impacts of operational conditions. Section 4 summarizes the key findings of this work.

## 2. Methodology

## 2.1. Reservoir model

In this section, a dual permeability 10,000 ft (L)  $\times$  10,000 ft (W)  $\times$  100 ft (H) reservoir simulation model was developed with a set of parameters according to the Barnett shale formation [44]. This heterogeneous reservoir with considering the natural fracture effect was developed based on the commercial compositional simulator *GEM* by CMG to solve a multi-component system [45,46]. The initial gas composition was assumed containing CH<sub>4</sub> only, and CO<sub>2</sub> and N<sub>2</sub> were defined as the injected gas components. The initial reservoir model was created and validated in the published work by Yu et al. [44], and then



(a) 2D top view of the reservoir

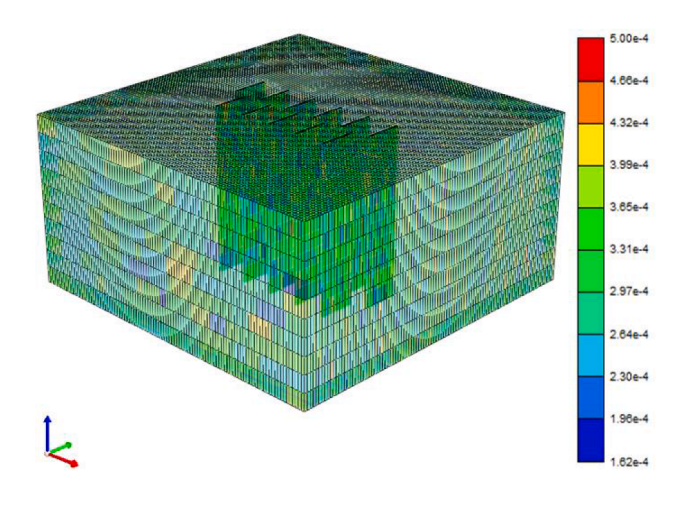


Fig. 1. Heterogeneous reservoir model with colors standing for horizontal matrix permeability.

(b) 3D view

the reservoir heterogeneity and the injection parameters were modified for this study. A relationship between permeability and porosity for both matrix and natural fractures was calculated based on the Kozeny-Carman equation with assumed average permeability and porosity from the literature [7,44,47]:

$$k = \alpha \cdot \frac{\phi^3}{(1 - \phi)^2} \tag{1}$$

where k is permeability [mD];  $\varphi$  is porosity [unitless];  $\alpha$  is a regression coefficient. With the known average permeability and porosity,  $\alpha$  can be calculated by equation (1). The porosity of each block was generated by Monte Carlo simulation with a normal distribution and average value. Therefore, the permeability of each block can be calculated by equation (1). The permeability and porosity of both matrix and fractures were calculated and input to CMG-GEM as described in Fig. 1 (a) and (b). The relative permeability for matrix and fractures can be found in Fig. 2 [36]. Two multistage horizontal hydraulic fractured wells were created as Fig. 1(a) shows. The space between these two wells is 1,000 ft, and the stage spacing and half-length were set at 1,000 and 500 ft, respectively. The detailed reservoir properties can be found in Table 1. Primary recovery lasted for 30 years with both wells serving as the producers with constant bottomhole pressure (BHP) assumed at 500 psi. The ESGR

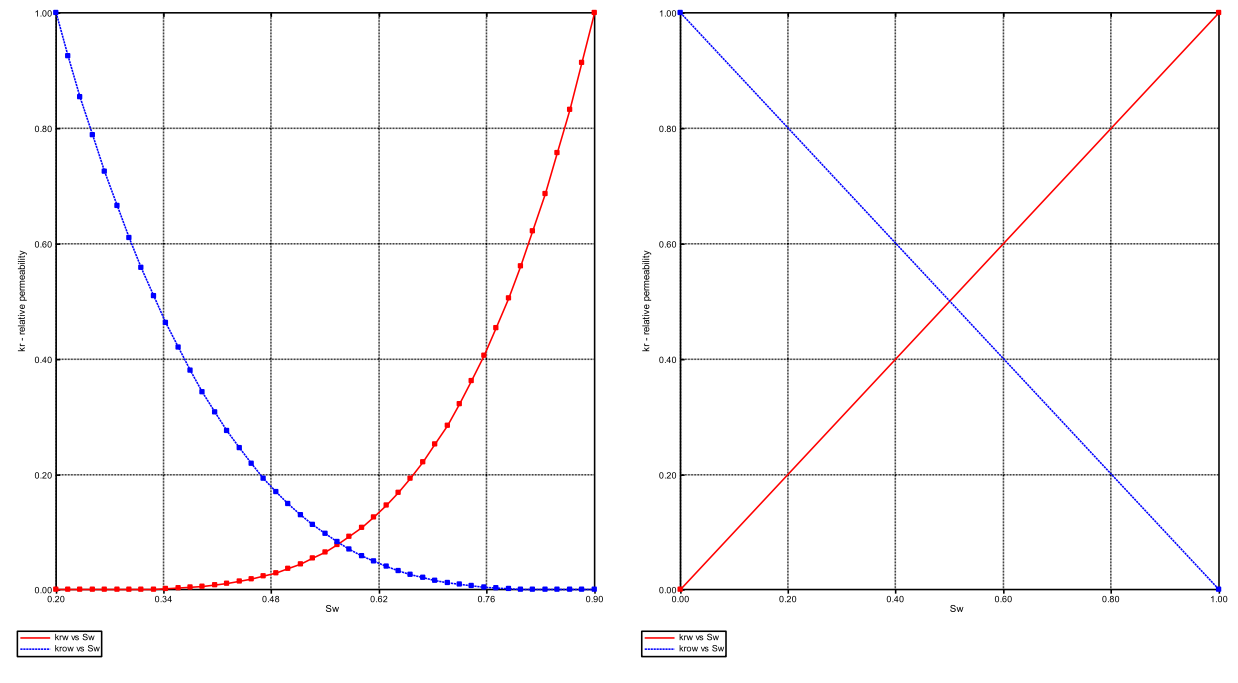


Fig. 2. Relative permeability curves for (a) matrix (left side) and (b) fractures (right side).

**Table 1**Input parameters for the reservoir model.

Reservoir Property [44,48]	Value	Unit
Depth – D	6481	ft
Thickness – H	100	ft
Average porosity matrix – $\varphi_m$	0.041	_
Average porosity fracture – $\varphi_f$	0.007	_
Average permeability matrix – $k_m$	0.0003	mD
Average permeability fracture – $k_f$	1.4	mD
Anisotropy	0.1	_
Natural fracture spacing i,j,k	0.5	ft
Initial Reservoir Temperature – T <sub>i</sub>	150	F
Initial Reservoir Pressure – P <sub>i</sub>	4500	psi
Well Property		
Stage spacing	1000	ft
Half length	500	ft
Well spacing	1000	ft
Gas Adsorption [37]		
N <sub>2</sub> Lamgmuir Pressure Constant – P <sub>L,N2</sub>	1087	psia
CH <sub>4</sub> Lamgmuir Pressure Constant – P <sub>L,CH4</sub>	1596	psia
CO <sub>2</sub> Lamgmuir Pressure Constant – P <sub>L,CO2</sub>	1254	psia
N <sub>2</sub> Lamgmuir Volume Constant – V <sub>L,N2</sub>	11.8	scf/ton
CH <sub>4</sub> Lamgmuir Volume Constant – V <sub>L,CH4</sub>	39.2	scf/ton
CO <sub>2</sub> Lamgmuir Volume Constant – V <sub>L,CO2</sub>	183.6	scf/ton

started from year 31 by shifting one producer to the injector (bottom one in Fig. 1(a)) with a constant injection rate at 0.4 MMSCF/day and injection pressure assumed not to exceed the initial reservoir pressure (i.e., 4,500 psi). The OGIP contained free gas and absorbed gas with the total volume of  $9.6 \times 10^4$  MMSCF. The maximum cumulative recovery factor of the primary production with both wells operating as the producers was estimated at 28.83 % over 50 years.

## 2.2. Gas adsorption and permeability evolution

Natural gas is usually trapped in three different thermodynamic states in shale: free compressed gas in intergranular porosity and fractures; absorbed gas on organic matters and clay materials; dissolved gas in kerogen [2]. Owing to different formations of shales, absorbed gas can account for 20 % to 85 % of total gas storage in shale reservoirs [49]. On the other hand,  $CO_2$  is preferentially absorbed over methane and

nitrogen on both inorganic and organic micropores [26,31,41]. Therefore, taking advantage of the competitive adsorption can unlock a higher natural gas recovery factor. The classical Langmuir isotherm is the most commonly model to evaluate a monolayer gas adsorption volume at pressure P for shale gas reservoirs as shown in Equation (2) [2,34,44,50,51]:

$$V(P) = \frac{V_L P}{P + P_L} \tag{2}$$

where V(P) is the gas adsorption volume at pressure P;  $V_L$  is the Langmuir volume constant corresponding to maximum adsorption capacity;  $P_L$  is the Langmuir pressure defining the curvature of an isotherm. Given the limitations of the classical Langmuir model, the BET model (Equation (3)) was developed to deal with multilayer adsorption [52]:

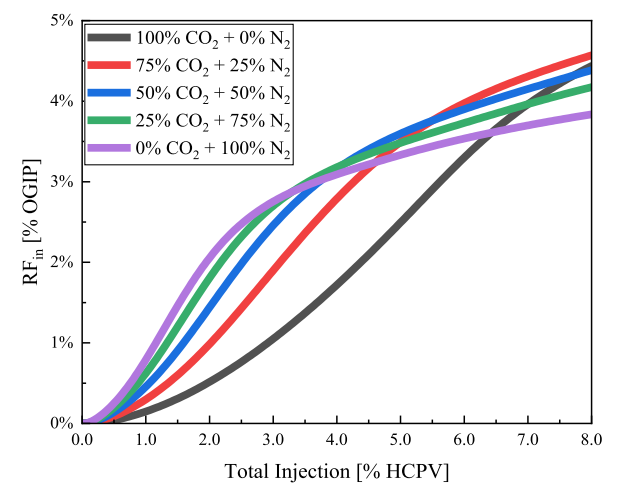
$$\frac{1}{V(\frac{p}{p_0} - 1)} = \frac{1}{V_{\rm m}c} + \frac{c - 1}{V_{\rm m}c} \left(\frac{P}{P_0}\right) \tag{3}$$

where  $P/P_0$  is the relative pressure;  $V_m$  is the monolayer adsorption capacity; c is a characteristic energy constant. The extended Langmuir model was used by CMG-GEM to consider the multicomponent adsorption under a heterogenous surface condition as shown in Equation (4) [53,54]:

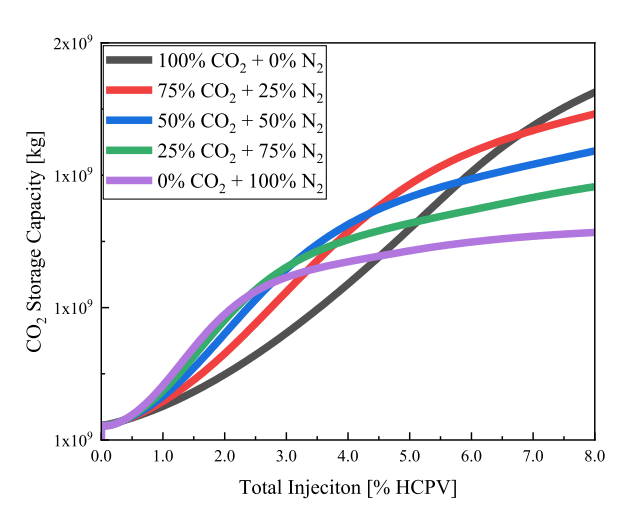
$$\omega_i = \frac{\omega_{i,\text{max}} B_i y_{i,aqu}}{1 + \sum_i B_j y_{i,aqu}} \tag{4}$$

where  $B_i$  is a parameter for a Langmuir isotherm relation;  $\omega_i$  indicates the moles of an adsorbed component per unit mass of rock;  $\omega_{i,\max}$  is the maximum moles of the adsorbed component i per unit mass of rock;  $y_{i,aqu}$  is the molar fraction of the adsorbed component i in the aqueous phase, where the aqueous phase is the gas phase for a shale gas reservoir as there is no other phases included in this study.

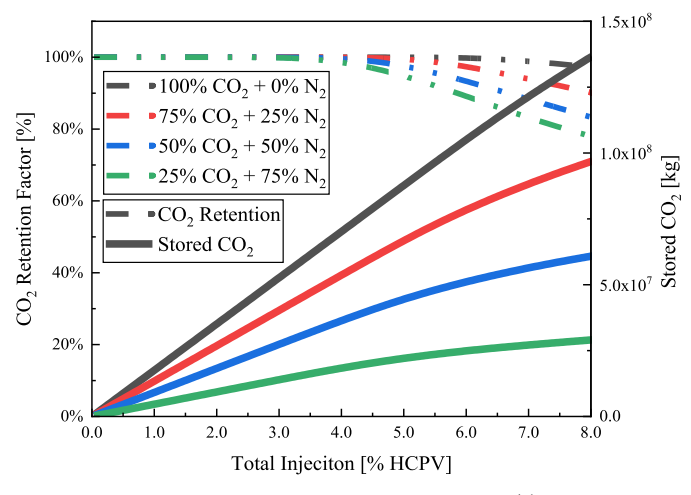
The permeability evolution described an effect of changing matrix and fracture permeability over time with gas injected to a shale gas reservoir. When injecting  $CO_2$ , the matrix permeability increases, and the fracture permeability decreases over time owing to the competitive adsorption  $CO_2$  over  $CH_4$  on shale triggering the matrix swell and fracture shrinkage. However, the injection of  $N_2$  will lead to a decreasing matrix permeability and increasing fracture permeability due to its



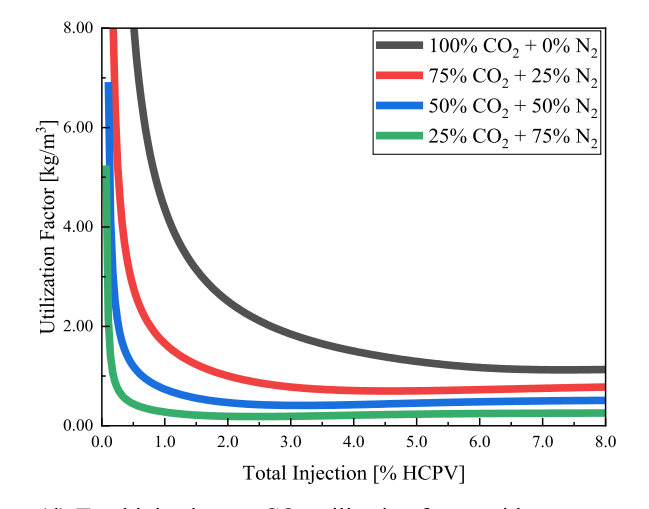
(a) Total Injection vs. RF<sub>in</sub> with respect to different CO<sub>2</sub>-N<sub>2</sub> ratio



(c) Total injection vs. CO<sub>2</sub> storage capacity with respect to different CO<sub>2</sub>-N<sub>2</sub> ratio



(b) Total injection vs. CO<sub>2</sub> retention and CO<sub>2</sub> stored with respect to different CO<sub>2</sub>-N<sub>2</sub> ratio



(d) Total injection vs.  $CO_2$  utilization factor with respect to different  $CO_2$ - $N_2$  ratio

Fig. 3. Impact of CO<sub>2</sub>-N<sub>2</sub> ratio.

effect of desorbing CH<sub>4</sub> by lowering its partial pressure and causing the matrix shrinkage and fracture widening [34].

## 2.3. Computational indicators

In this section, the calculational methods were demonstrated from the perspectives of shale gas recovery and  $CO_2$  sequestration. To evaluate the performance of shale gas recovery, the RF [%] was adopted by taking a ratio of cumulative gas production over the OGIP as shown in Equation (5):

$$RF_{in} = \frac{P_{cum} - E[P_{cum}]}{OGIP} \tag{5}$$

where  $P_{ctum}$  is the cumulative shale gas produced and  $E[P_{ctum}]$  is the expected cumulative shale gas production without ESGR. The total gases injection including  $CO_2$  and  $N_2$  at the ESGR stage is presented as the percentage of a hydrocarbon pore volume (HCPV) at the surface condition defined by Equation (6):

$$HCPV_{inj} = \frac{\sum V_{\alpha,sc}}{V_{HCPV}} \tag{6}$$

where  $V_{\alpha,sc}$  is the volume of the injected  $\alpha$  gases at the surface condition, where  $\alpha$  can include  $CO_2$  and  $N_2$ ;  $V_{HCPV}$  is the total HCPV; and  $HCPV_{inj}$  is the unitless injected gas in the HCPV scale.

Besides the shale gas recovery, CO2 sequestration is another major consideration in the context of greenhouse gases emission reduction. As described in the previous sections, injecting CO2 into shale gas reservoirs can not only improve the gas recovery, but also permanently sequestrate CO<sub>2</sub> to mitigate the CO<sub>2</sub> emissions. In addition, successful CO<sub>2</sub> storage can earn a carbon credit to improve the revenues of a project. According to IEA, the carbon price will rise CAD \$15 per tonne annually to CAD \$170 per tonne by 2030 [55]. In this work, the CO2 storage capacity and CO2 retention factor were considered to evaluate the performance of CO<sub>2</sub> sequestration in a reservoir as illustrated in Equations (7) and (8), respectively. The CO2 storage capacity can be calculated based on the modified USDOE method with considering contributions from both free trapping and adsorption mechanisms; an impact of hysteresis was neglected in this study [40,56–59]. The total volume that can be occupied by CO2 is the volume of free trapped CO2 plus the additional absorbed CO2 in a shale formation owing to the competitive adsorption effect and deducting the volume that is occupied by nitrogen. The retention factor of CO<sub>2</sub> in percentage can be calculated by taking a ratio of retained CO<sub>2</sub> over total injected CO<sub>2</sub> as illustrated in Equation (8). Both Equations (7) and (8) are calculated at the standard conditions:

$$M_{CO_2} = \rho_{CO_2,sc} \cdot \left( RF_{cum} \times OGIP + V_{CO_2,absorbed} - V_{CH_4,absorbed} - V_{N_2,retained} \right) \tag{7}$$

$$R_{CO_2} = \frac{M_{CO_2,inj} - M_{CO_2,prod}}{M_{CO_2,ini}} \tag{8}$$

The utilization factor normalized the recovery efficiency of natural gas production by applying  $CO_2$ . It defines an amount of  $CO_2$  utilized to recover a unit volume of natural gas. Since  $CO_2$  is an expensive source for field applications decades ago, minimizing the  $CO_2$  usage was always expected to maximize project revenues [60,61]. However, with a large-scale implementation of an emission trading market, the industrial direction will shift to store  $CO_2$  as much as possible so that a carbon credit can be received to maximize the project revenues. Hence, the utilization factor can be given in Equation (9):

$$UF_{CO_2} = \frac{M_{CO_2,stored}}{RF_{in} \times OGIP} \tag{9}$$

where  $UF_{CO2}$  is the utilization factor [M/L<sup>3</sup>];  $RF_{in}$  is the incremental recovery factor. The  $UF_{CO2}$  demonstrated that an amount of  $CO_2$  was stored in mass when recovering an additional volume of natural gas from a reservoir. We used the mass unit of  $CO_2$  and the volumetric unit of natural gas as the unit market prices for  $CO_2$  and natural gas are in ton and  $m^3$ , respectively. The utilization factor can be adopted to describe the reservoir performance from both resource recovery and  $CO_2$  sequestration perspectives.

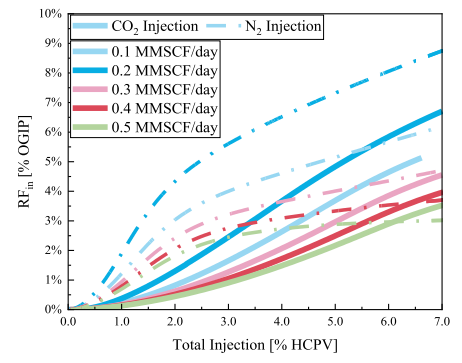
#### 3. Result and discussion

#### 3.1. Continuous flooding

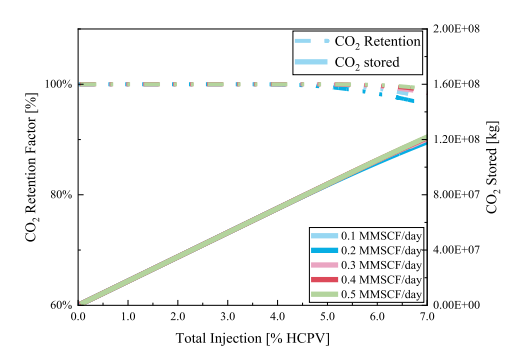
In this section, an optimal  $\mathrm{CO_2\text{-}N_2}$  ratio and injection rate were investigated based on a series of reservoir simulations. The constant injection rate operation was assumed at the ESGR stage with the injector BHP not exceeding its initial reservoir pressure. With the total injection of a gas mixture at 8.0 HCPV, the  $RF_{in}$  of shale gas,  $\mathrm{CO_2}$  storage capacity,  $\mathrm{CO_2}$  retention factor and utilization factor were compared for all scenarios.

#### 3.1.1. Impact of a CO<sub>2</sub>-N<sub>2</sub> ratio

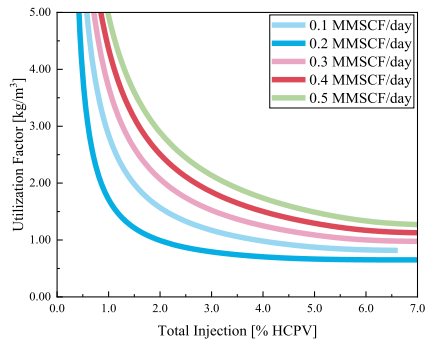
As illustrated in Fig. 3, Fig. 3(a) demonstrated the incremental recovery factor after the gas mixture is injected into the reservoir. As a result, the pure application of nitrogen has a better performance at the early stage owing to its impact on increasing the matrix permeability so that CH<sub>4</sub> molecules can flow to fractures. However, due to the smallest adsorption effect of N2 compared to CH4 and CO2, the recovered amount of absorbed CH<sub>4</sub> is limited, and the breakthrough time of N<sub>2</sub> injection is shorter compared to the CO2 injection. The injection of a CO2-N2 mixture can postpone the breakthrough time compared with pure N2 injection and a larger adsorption effect of CO2 can recover the absorbed CH<sub>4</sub> with the help of N<sub>2</sub> lowering the partial pressure of CH<sub>4</sub>. We further observed that the injected CO2 was absorbed to the shale formation at an early stage of the injection so that the matrix permeability was not increased, and hence the incremental gas recovery was maintained at a lower factor. Therefore, the pure CO2 injection can perform better at a late stage because of the increasing fracture permeability and much more absorbed CH<sub>4</sub> replaced by CO<sub>2</sub> owing to the competitive adsorption mechanism. Fig. 3(b) showed the evaluation of CO<sub>2</sub> sequestration, and the results illustrated that all injected CO<sub>2</sub> can be stored as long as the breakthrough time is not achieved. A higher concentration of CO<sub>2</sub> can trigger a slower breakthrough time. The CO<sub>2</sub> storage capacity curves (Fig. 3(c)) were in the same shape as  $RF_{in}$  due to a correlation between the storage capacity and cumulative recovery factor. Thus, the N2 application will result in less  $CO_2$  storage capacity and a shorter



(a) Total injection vs. RFin with respect to different injection rate of CO2 and N2



(b) Total injection vs. CO<sub>2</sub> retention & CO<sub>2</sub> stored with different CO<sub>2</sub> injection rate



(c) Total injection vs. CO2 utilization factor with respect to different CO2 injection rate

Fig. 4. The impacts of an injection rate.

breakthrough period of injected gas. The cumulative  $CO_2$  production is positively correlated with the  $N_2$  percentage. However, it can improve the methane recovery factor at an early stage for shale reservoirs. To analyze from both natural gas recovery and  $CO_2$  sequestrating perspectives, we adopted the utilization factor of  $CO_2$  as shown in Fig. 3(d). The utilization factor declines rapidly starting from the injection of gas and approximates a constant value after the injected gas breakthroughs. The final utilization factor of  $CO_2$  is in a range from 0.26 to 1.16 kg/m³ increasing with the  $CO_2$  purity indicating that 1 m³ of  $CH_4$  recovered can store up to 1.16 kg  $CO_2$ . Overall, the injection of 75 %  $CO_2$  plus 25 %  $CO_2$ 0 less than 7.0 HCPV can reach the highest gas recovery and  $CO_2$ 1 storage goals with the  $CO_2$ 1 utilization factor at 0.8 kg/m³ according to our observations.

#### 3.1.2. Impact of an injection rate

Besides the  $CO_2$ - $N_2$  ratio, the variation of an injection rate can also significantly influence the natural gas recovery as well as the  $CO_2$  storage according to the results in Fig. 4. The injection rates in a range from 0.1 to 0.5 MMSCF/day were studied accordingly to address the impact of changing an injection rate. Increasing an injection rate can improve the shale gas recovery before the injected gas breakthroughs

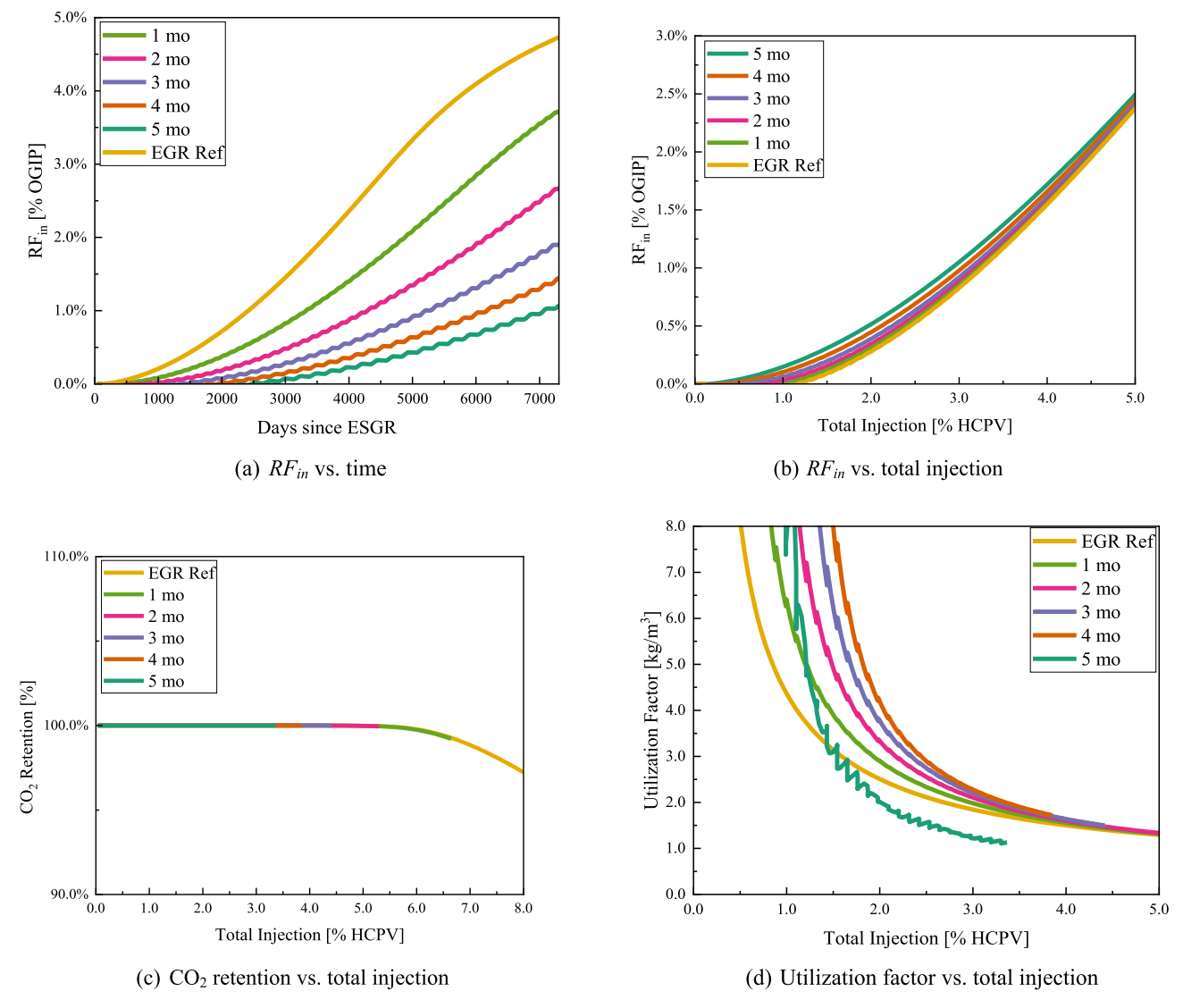
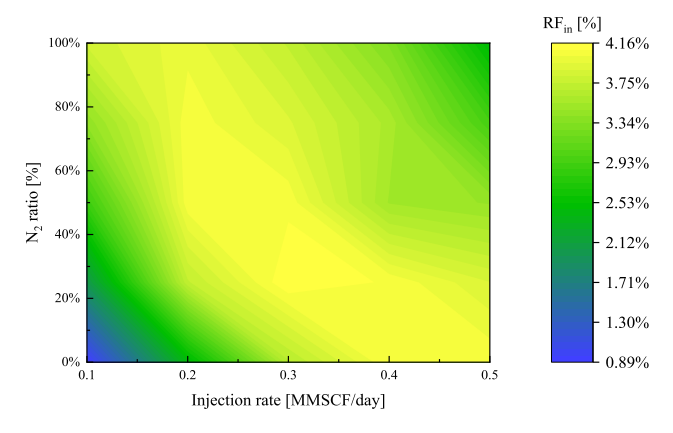


Fig. 5. Performance comparison of cyclic flooding scenarios.

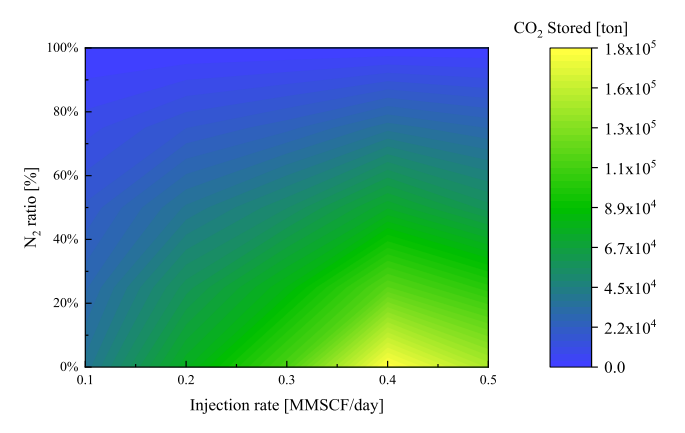
within the same time frame. However, when controlling the total mass of injected gas there was a threshold injection rate at which a higher injection rate led to a lower recovery factor. For example, the optimal injection rate in this study was 0.2 MMSCF/day for both pure CO<sub>2</sub> and N<sub>2</sub> as the ESGR fluids showed as the solid and dash-dot lines in Fig. 4(a), respectively, with the same amount of total injection fluids. The reason is that a higher injection rate requires a higher BHP of the injector and hence reduces breakthrough time owing to the higher reservoir pressure and permeability. Thus, the production rate of CH<sub>4</sub> declines rapidly after the injected gas breakthroughs as more CO2 was being produced, and result in a lower sweep efficiency of CH<sub>4</sub> afterward. Hence, a longer breakthrough time can secure a higher recovery factor. On the other hand, if the injection rate was extremely low, the injected gas remained immobile so that the free CH<sub>4</sub> molecules cannot flow to the producer. Additionally, the fracture permeability cannot be effectively improved with a great increasing rate of gases beyond the threshold injection rate. Therefore, the natural gas cannot be extracted. The results of CO2 retention and the amount of CO<sub>2</sub> stored (Fig. 4(b)) were similar as the previous results stated. As long as the breakthrough point is not reached, the injected CO<sub>2</sub> can be successfully sequestrated. The CO<sub>2</sub> utilization factors were in a range from 0.65 to 1.43 m<sup>3</sup>/kg. A higher injection rate can store more CO2 per cubic meter of CH4 recovered, but it also indicated less efficiency of CO2 utilization. To sum up, the 0.2 MMSCF can not only recover the most amount of  $CH_4$  but also effectively store  $CO_2$  with a utilization factor of 0.65 kg/m $^3$  compared with other scenarios for pure  $CO_2$ .

## 3.2. Cyclic flooding

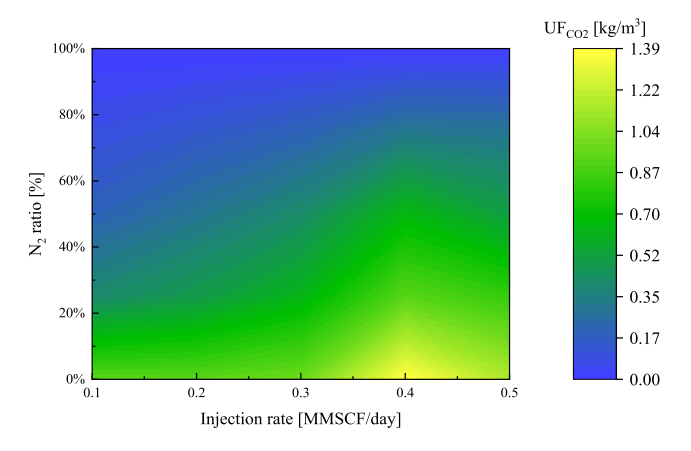
In this section, we studied five cyclic injection scenarios to address the impact of soaking time on the reservoir performance. As known, a Huff and Puff (HnP) process can be applied to shale reservoirs and the soaking time can significantly impact a recovery factor [62]. To analyze the impact of a soaking period on the shale gas recovery and CO2 sequestration, we developed the five cyclic injection scenarios with a soaking period from 1 to 5 months as shown in Fig. 5. For each scenario, the producer and injector are alternatively shut in for a specific time so that the soaking impact of a CO<sub>2</sub>-N<sub>2</sub> mixture can be addressed. The optimal CO<sub>2</sub>-N<sub>2</sub> mixture with a ratio of 75 % CO<sub>2</sub> plus 25 % N<sub>2</sub> was deployed, as proven in Section 3.1. According to Fig. 5(a), a longer soaking period requires longer time to inject the same amount of gas to the reservoir and trigger a lower RFin within the same timeframe. However, Fig. 5(b) shows that when the total injections were same, a longer period can improve the shale gas recovery as more absorbed CH<sub>4</sub> can be extracted especially in an early stage of operation. With the total injected fluid increasing, the RFin of each scenario was approximate to







#### (b) The optimization solution for CO<sub>2</sub> sequestration



(c) The optimization solution for CO2 utilization factor

Fig. 6. Optimization scheme from engineering perspective.

each other as the impact of a soaking time decays. Fig. 5(c) shows that a soaking period has no impact on the breakthrough time as all scenarios were sharing the same curve of  $CO_2$  retention. Similarly, the utilization factor of  $CO_2$  was different at an early stage of the simulation owing to the distinct recovery factors and approached the same value with injecting an increasing amount of the gas mixture. Understanding the impact of a soaking period can provide a sense to formulate an economic evaluation of operation as to whether it is worthwhile to recover an extra amount of  $CH_4$  by an impact of the soaking mechanism in a longer timeframe with less total injected  $CO_2$ - $N_2$  mixture. In brief, the soaking period of injected gas had limited impact on both ESGR and  $CO_2$  sequestration according to our simulation results.

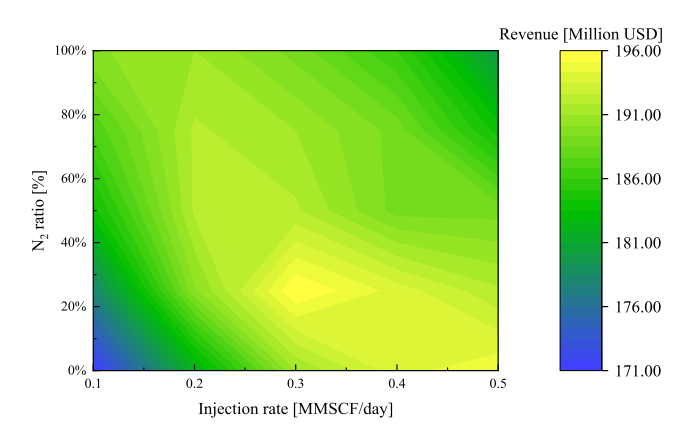


Fig. 7. Optimization scheme of project revenues.

#### 3.3. Optimized schemes

In this section, an optimized operation scheme was determined based on simulations using the CMOST module. An injection rate, CO<sub>2</sub>-N<sub>2</sub> ratio, and soaking period were considered initially as the optimizers. However, as discussed in the previous section, a soaking period has no impact after 4.0 HCPV of injected gases. The cyclic injection schemes were eliminated in this section and the continuous ESGR flooding was assumed for over 40 years so that at least 4.0 HCPV of a gas mixture can be injected to the reservoir. By selecting different combinations of an injection rate and a CO2-N2 ratio, the optimal ESGR and CO2 sequestration performance can be determined according to Fig. 6 (a)-(c) with  $\sim 100$  simulation cases performed by CMOST. In Figs. 6 and 7, a N<sub>2</sub> ratio defines the percentage of N2 of the injected gas. For example, the 100 % N<sub>2</sub> ratio indicates that the injected gas is comprised of N<sub>2</sub> only, whereas the 0 % N<sub>2</sub> ratio indicates that the injected gas is comprised of CO<sub>2</sub> only. As shown in Fig. 6(a), the highest RF<sub>in</sub> can reach 4.16 % by injecting 30 % N<sub>2</sub> and 70 % CO<sub>2</sub> at an injection rate of 0.3 MMSCF/day. A higher injection rate with a higher N<sub>2</sub> ratio result in an inefficient recovery factor, as the absorbed natural gas cannot be displaced to the producer. Furthermore, a low injection rate and high purity of CO<sub>2</sub> cannot effectively achieve the greatest ESGR recovery goal, as the matrix permeability was not increasing owing to a larger adsorption capacity of CO<sub>2</sub>. Fig. 6(b) illustrated the performance of CO<sub>2</sub> sequestration by estimating the total amount of CO2 stored to the reservoir. As discussed in the previous sections, the injected CO<sub>2</sub> can be successfully stored in the reservoir before the gas breakthrough. A larger injection rate can result in a shorter breakthrough time. Once the injected gas was produced, the decreasing CO2 retention factor suggested that the storage efficiency was decreasing. An optimal combination to store CO2 associated with the ESGR process was at an injection rate of 0.4 MMSCF/day and 100 % CO<sub>2</sub> concentration of the injected gas. The result proved that the maximum of 180 thousand tonnes CO2 can be stored in the reservoir according to the simulations. The CO2 utilization factor can be calculated consequently as shown in Fig. 6(c). Owing to the greatest CO2 storage, the pure CO2 injection at a rate of 0.4 MMSCF/day also leads to the highest utilization factor, which is 1.39 kg/m<sup>3</sup> indicating that one cubic meter of natural gas recovery can contribute to 1.39 kg of CO<sub>2</sub> storage during the ESGR process. However, a higher utilization factor also suggests the less efficiency of CO<sub>2</sub>. Thus, a project optimization scheme should not only consider the reservoir performance but also economic revenues.

The economic revenues without considering the time value of money (a discount rate) can be estimated by summing up the sale revenues of natural gas plus receiving a tax credit for the carbon sequestration as in Equation (10):

$$Revenue = p_{NG} \times Q_{NG} + p_{CO_2} \times Q_{CO_2}$$
 (10)

where  $p_{NG}$  is the unit price of natural gas assumed at \$6.85/MCF in 2022 USD according to the U.S. energy information agency (USEIA);  $p_{CO2}$  is the carbon price for geologically sequestrated CO<sub>2</sub> with EOR (enhanced oil recovery) at the value of \$25/ton in 2022 USD according to 45Q;  $Q_{NG}$  and  $Q_{CO2}$  are the cumulative produced CH<sub>4</sub> and cumulative stored CO<sub>2</sub>, respectively, according to numerical simulations [63,64]. Fig. 7 illustrates the revenue variation with combinations of an injection rate and a CO<sub>2</sub>-N<sub>2</sub> ratio. As a result, the highest total revenue requires the largest amount of natural gas production and storing CO<sub>2</sub> as much as possible in the current price scenario. A successful implementation of CO<sub>2</sub>-N<sub>2</sub> ESGR can earn up to 7 % to 22 % more revenues for a project, and 13 % of the additional revenues is from the carbon credit. Therefore, under the current carbon price, the CO<sub>2</sub> sequestration can significantly improve the revenues of an ESGR project. By selecting the optimal operation strategy, the revenues of a project can be improved by 15 %.

#### 4. Conclusions

In this work, we deployed the *GEM* and CMOST of CMG to investigate the feasibility of a  $\rm CO_2\text{-}N_2$  mixture for the purpose of ESGR and proposed the optimized operating strategies to overcome the dual challenges of maximizing the natural gas recovery as well as permanently sequestrating  $\rm CO_2$  in shale formations. A total of 120 simulation scenarios were conducted to address the impacts of a  $\rm CO_2\text{-}N_2$  ratio, injection rate and cyclic soaking period, and an optimal combination of a  $\rm CO_2\text{-}N_2$  ratio and an injection rate was concluded to maximize project revenues consequently. The competitive adsorption mechanism was considered during an ESGR phase, and the performance of a reservoir was evaluated from the natural gas recovery and  $\rm CO_2$  sequestration perspectives. The limitation of this study includes that the  $\rm CO_2$  storage mechanisms do not include a mineralization process. As the results indicated, we summarize the following contributions.

- A larger concentration of N<sub>2</sub> corresponds to a higher methane recovery factor at an early stage but caused less amount of CO<sub>2</sub> storage owing to a shorter breakthrough period.
- (2) A higher injection rate does not always indicate that a greater amount of natural gas can be recovered associated with great performance of CO<sub>2</sub> sequestration.
- (3) A soaking period only impacts the ESGR performance at an early stage and has no impact to both gas recovery and CO<sub>2</sub> sequestration in a long term.
- (4) An optimized scheme can be determined by varying an injection rate and a  $\rm CO_2\text{-}N_2$  ratio simultaneously to achieve the max revenues with earning a carbon credit at a significant level. In our case, the optimal combination is 70 %  $\rm CO_2$  plus 30 %  $\rm N_2$  at an injection rate of 0.33 MMSCF/day with the continuous flooding.
- (5) The optimized scheme shows that a project can earn up to 22 % more revenues under the current carbon tax policy. By controlling an injection rate and a gas mixture ratio, the project revenues can be improved by 15 %.

## **Declaration of Competing Interest**

The authors declare that they have no known competing financial interests or personal relationships that could have appeared to influence the work reported in this paper.

## Data availability

Data will be made available on request.

## Acknowledgements

This research has been made possible by contributions from the

Natural Sciences and Engineering Research Council (NSERC)/Energi Simulation Industrial Research Chair in Reservoir Simulation and the Alberta Innovates (iCore) Chair in Reservoir Modeling.

#### References

- [1] IEA. World Energy Outlook 2021. IEA, Paris, 2021.
- [2] Yang Y, Liu S. Review of shale gas sorption and its models. Energy Fuels 2020.
- [3] Jarvie DM, Hill RJ, Ruble TE, Pollastro RM. Unconventional shale-gas systems: The Mississippian Barnett Shale of north-central Texas as one model for thermogenic shale-gas assessment. AAPG Bull 2007;91:475–99.
- [4] Sakhaee-Pour A, Bryant SL. Gas permeability of shale. SPE Reservoir Eval Eng 2012:15:401–9.
- [5] Wu K, Chen Z. Real gas transport through complex nanopores of shale gas reservoirs. SPE Europec featured at 78th EAGE Conference and Exhibition. Society of Petroleum Engineers, Vienna, Austria, 2016. p. 22.
- [6] Wang R, Zhang K, Detpunyawat P, Cao J, Zhan J. Analytical solution of matrix permeability of organic-rich shale. International Petroleum Technology Conference 2016.
- [7] Zhan J, Yuan Q, Fogwill A, Cai H, Hejazi H, Chen Z, et al. A systematic reservoir simulation study on assessing the feasibility of CO2 sequestration in shale gas reservoir with potential enhanced gas recovery. Carbon Management Technology Conference. Carbon Management Technology Conference, Houston, Texas, USA, 2017. p. 12.
- [8] Yang S. Coupled studies of shale reservoirs characterization and simulation; 2018.
- [9] Liu X, Zhang L, Zhao Y, He X, Wu J, Su S. Shale gas transport in nanopores: contribution of different transport mechanisms and influencing factors. Energy Fuels 2021;35:2033–47.
- [10] IEA. Net Zero by 2050. IEA, Paris; 2021.
- [11] IPCC. Special report on carbon dioxide capture and storage. Cambridge, UK/New York, NY, USA, 2005.
- [12] IPCC. Climate change 2022: mitigation of climate change; 2022.
- [13] Clemens T, Wit K. CO2 enhanced gas recovery studied for an example gas reservoir; 2002.
- [14] Lackner KS. A guide to CO2 sequestration. Science 2003;300:1677-8.
- [15] Li Z, Dong M, Li S, Huang S. CO2 sequestration in depleted oil and gas reservoirs—caprock characterization and storage capacity. Energy Convers Manage 2006:47:1372–82.
- [16] Bachu S. CO2 storage in geological media: Role, means, status and barriers to deployment. Prog Energy Combust Sci 2008;34:254–73.
- [17] Faltinson JE, Gunter B. Net CO2 Stored in North American EOR Projects. J Can Pet Technol 2011;50:55–60.
- [18] Seyyedsar SM, Farzaneh SA, Sohrabi M. Enhanced heavy oil recovery by intermittent CO2 injection; 2015.
- [19] Wang X, van 't Veld K, Marcy P, Huzurbazar S, Alvarado V. Economic cooptimization of oil recovery and CO2 sequestration. Appl Energy. 222 (2018) 132-47
- [20] Lake LW, Lotfollahi M, Bryant SL. Fifty years of field observations: Lessons for CO2 storage from CO2 enhanced oil recovery; 2018.
- [21] Wang H, Rezaee R. CO2 storage with enhanced gas recovery CS-EGR in conventional and unconventional gas reservoirs in Australia; 2020.
- [22] Lee KS, Cho J, Lee JH. CO2 storage coupled with enhanced oil recovery. Springer International Publishing 2020.
- [23] Arnaut M, Vulin D, José García Lamberg G, Jukić L. Simulation analysis of CO2-EOR process and feasibility of CO2 storage during EOR. Energies. 14 (2021).
- [24] DeAngelo J, Azevedo I, Bistline J, Clarke L, Luderer G, Byers E, et al. Energy systems in scenarios at net-zero CO2 emissions. Nat Commun 2021;12.
- [25] Ou Y, Roney C, Alsalam J, Calvin K, Creason J, Edmonds J, et al. Deep mitigation of CO2 and non-CO2 greenhouse gases toward 1.5 degrees C and 2 degrees C futures. Nat Commun 2021;12:6245.
- [26] Liu J, Xie L, Elsworth D, Gan Q. CO2/CH4 competitive adsorption in shale: implications for enhancement in gas production and reduction in carbon emissions. Environ Sci Technol 2019.
- [27] Liu D, Li Y, Yang S, Agarwal RK. CO2 sequestration with enhanced shale gas recovery. Energy Sources Part A 2019:1–11.
- [28] Mohagheghian E. Numerical modeling of multi-mechanistic gas production from shale reservoirs; 2020.
- [29] Grinestaff G, Barden C, Miller J, Franklin W, Barden C, Ding E. Evaluation of eagle ford cyclic gas injection EOR: field results and economics; 2020.
- [30] Berawala DS, Østebø Andersen P. Fracture-matrix modelling of CO2 enhanced shale gas recovery in compressible shale. SPE Asia Pacific Oil & Gas Conference and Exhibition. 2020.
- [31] Lyu Q, Tan J, Li L, Ju Y, Busch A, Wood D, et al. The role of supercritical carbon dioxide for recovery of shale gas and sequestration in gas shale reservoirs. Energy Environ Sci 2021.
- [32] Yang Y, Liu S. Estimation and modeling of pressure-dependent gas diffusion coefficient for coal: A fractal theory-based approach. Fuel 2019;253:588–606.
- [33] Yang Y, Liu S. Integrated modeling of multi-scale transport in coal and its application for coalbed methane recovery. Fuel 2021;300.
- [34] Li Z, Elsworth D. Controls of CO2–N2 gas flood ratios on enhanced shale gas recovery and ultimate CO2 sequestration. J Petroleum Sci Eng 2019;179:1037–45.
- [35] Psarras P, Holmes R, Vishal V, Wilcox J. Methane and CO2 adsorption capacities of kerogen in the eagle ford shale from molecular simulation. Acc Chem Res 2017;50: 1818–28.

- [36] Zhan J, Soo E, Fogwill A, Cheng S, Cai H, Zhang K, et al. A systematic reservoir simulation study on assessing the feasibility of CO2 sequestration in liquid-rich shale gas reservoirs with potential enhanced gas recovery; 2018.
- [37] Vermylen JP. Geomechanical studies of the Barnett Shale, Texas. USA: Stanford University; 2011.
- [38] Cai Y, Dahi Taleghani A. Pursuing improved flowback recovery after hydraulic fracturing. SPE Eastern Regional Meeting 2019.
- [39] Dahi Taleghani A, Cai Y, Pouya A. Fracture closure modes during flowback from hydraulic fractures. Int J Numer Anal Methods Geomech 44; 2020: 1695-704.
- [40] USDOE. Carbon storage atlas fifth edition: national energy technology laboratory; 2015.
- [41] Qin C, Jiang Y, Zhou J, Song X, Liu Z, Li D, et al. Effect of supercritical CO2 extraction on CO2/CH4 competitive adsorption in Yanchang shale. Chem Eng J 2021:412.
- [42] Zhou S, Xue H, Ning Y, Guo W, Zhang Q. Experimental study of supercritical methane adsorption in Longmaxi shale: Insights into the density of adsorbed methane. Fuel 2018;211:140–8.
- [43] Xie W, Wang M, Chen S, Vandeginste V, Yu Z, Wang H. Effects of gas components, reservoir property and pore structure of shale gas reservoir on the competitive adsorption behavior of CO2 and CH4. Energy 2022;254.
- [44] Yu W, Al-Shalabi EW, Sepehrnoori K. A sensitivity study of potential CO2 injection for enhanced gas recovery in Barnett shale reservoirs. SPE Unconventional Resources Conference 2014.
- [45] Chen Z. Reservoir simulation mathematical techniques in oil recovery. Society for Industrial and Applied Mathematics, 2007.
- [46] CMG-GEM. [Computer Software]. Calgary, AB Canada; 2020.
- [47] Costa A. Permeability-porosity relationship: A reexamination of the Kozeny-Carman equation based on a fractal pore-space geometry assumption. Geophys Res Lett 2006:33
- [48] Palmer ID, Moschovidis ZA, Cameron JR. Modeling shear failure and stimulation of the Barnett shale after hydraulic fracturing. SPE Hydraulic Fracturing Technology Conference 2007.
- [49] Curtis JB. Fractured shale-gas systems. AAPG Bull 2002;86:1921-38.
- [50] Langmuir I. The adsorption of gases on plane surfaces of glass, mica and platinum. J Am Chem Soc 1918;40:1361–403.

- [51] Yang Y, Liu S, Clarkson C. Quantification of temperature-dependent sorption isotherms in shale gas reservoirs: experiment and theory. SPE J 2022:1–19.
- [52] Brunauer S, Emmett PH, Teller E. Adsorption of gases in multimolecular layers. J Am Chem Soc 1938;60:309–19.
- [53] Hall FE, Chunhe Z, Gasem KAM, Robinson Jr RL, Dan Y. Adsorption of pure methane, nitrogen, and carbon dioxide and their binary mixtures on wet fruitland coal. SPE Eastern Regional Meeting 1994.
- [54] Arri LE, Yee D, Morgan WD, Jeansonne MW. Modeling coalbed methane production with binary gas sorption. SPE Rocky Mountain Regional Meeting 1992.
- [55] IEA. Canada 2022. IEA, Paris, 2022.
- [56] V. Vishal, T.N. Singh. Geologic Carbon Sequestration: Understanding Reservoir Behavior. Springer International Publishing; 2016.
- [57] Bachu S, Bonijoly D, Bradshaw J, Burruss R, Holloway S, Christensen NP, et al. CO2 storage capacity estimation: Methodology and gaps. Int J Greenhouse Gas Control 2007;1(4):430–43.
- [58] Levine JS, Fukai I, Soeder DJ, Bromhal G, Dilmore RM, Guthrie GD, et al. DOE NETL methodology for estimating the prospective CO2 storage resource of shales at the national and regional scale. Int J Greenhouse Gas Control 2016;51:81–94.
- [59] Myshakin EM, Singh H, Sanguinito S, Bromhal G, Goodman AL. Numerical estimations of storage efficiency for the prospective CO2 storage resource of shales. Int J Greenhouse Gas Control 2018;76:24–31.
- [60] Al-Hasami A, Ren S, Tohidi B. CO2 injection for enhanced gas recovery and geostorage: reservoir simulation and economics; 2005.
- [61] Liu F, Ellett K, Xiao Y, Rupp JA. Assessing the feasibility of CO2 storage in the New Albany Shale (Devonian–Mississippian) with potential enhanced gas recovery using reservoir simulation. Int J Greenhouse Gas Control 2013;17:111–26.
- [62] Wang M, Wang L, Zhou W, Yu W. Lean gas Huff and Puff process for Eagle Ford Shale: Methane adsorption and gas trapping effects on EOR. Fuel 2019;248: 143-51.
- [63] EIA. United States Natural Gas Industrial Price. U.S. Energy Information Administration; 2022.
- [64] CRS. The tax credit for carbon sequestration (Section 45Q). U.S. Congressional Research Service; 2021.